ANALYSIS OF STATIC AND DYNAMIC AEROELASTIC CHARACTERISTICS OF AIRPLANE IN TRANSONIC FLOW

S. Kuzmina, O. Karas, F. Ishmuratov, M. Zichenkov, V. Chedrik
Central Aerohydrodynamic Institute (TsAGI), Zhukovsky, Russia
kuzmina@tsagi.ru

Keywords: *aeroelasticity, transonic flow, flutter, computation code*

Abstract

This paper describes the method developed in TsAGI for taking into account specific responses of an elastic airplane in transonic flow. For the analysis of strength, static and dynamic aeroelasticity characteristics the mathematical model of an elastic airplane is created in the ARGON system. New approach is based on Transonic Time-Harmonic Code for aeroelastic application. Linear flutter analysis in the frequency domain is supplemented with an effective algorithm/procedure of aerodynamic influence coefficients computation using time-harmonic solutions of the Euler equations in transonic viscous flow. It is available for rather complex airplane configurations.

1 Introduction

Industrial prediction of aeroelastic characteristics in transonic flow taking into account separated flow condition with shock boundary layer interaction is really relevant for flying vehicles of different types. For modern transport and passenger airplanes the transonic flight regime is critical in view of the necessity to ensure the safety from such aeroelasticity phenomena as flutter, limit cycle oscillations, aeroservoelastic instability, static stability and controllability, aeroelastic divergence of lifting surfaces and controls reversal. Therefore it is important to perform an airplane aeroelastic analysis for complete flight envelope including critical transonic regime [1].

Till now the majority of industrial practical numerical studies of airplane aeroelasticity characteristics are conducted mainly with the use of linear aerodynamic methods. As a rule the classical Doublet-Lattice Method (DLM) and several variants of panel methods are used. The necessity of an aerodynamic characteristic linearization has also another reason: application of effective methods in a stability analysis of complex linear dynamic systems.

In many aeronautical research centers for computation of aerodynamic forces accurate tools based on solution of the Euler and Navier-Stoks equations are now being developed. The Euler and Navier-Stoks solvers had recently been used mainly for an aerodynamic airplane design, but now these solvers server as tools for aeroelastic simulations more and more frequently. Many promising methods have been developed in this direction during the last 20 years. Some of them are based on boundary layer coupled time-domain computation fluid dynamics (CFD), for example the methods using Full Potential Theory [2] or Euler equation [3]. Other methods are linearized frequency domain CFD, mainly for unsteady Euler and Navier-Stoks equations [4]. It is also worth noting of the so called CFD-DLM correction methods, which are an extension of DLM to transonic and viscous flow [5]. A review of these methods is given in [6]. Many efforts are still made for their further improvement in the direction of the development of faster unsteady CFD methods. Improvement of an effectiveness of computational algorithms and grids generations, progress in computing power allow complex airplane configurations to be analyzed using a

variety of the Euler and Navier–Stokes solvers. However applications of these methods are restricted in the case of multidisciplinary airplane design and optimization where computations of aeroelastic characteristics have to be carried out many times for great number of variants and parameters of an airplane structure.

During the past decades, TsAGI has improved its aeroelasticity computation strategy by the use of the new CFD solver TTHC (Transonic Time-Harmonic Code), which was developed on the basis of a finite difference solution of the small disturbance unsteady Euler equations with a viscosity model (Blwf100 solver). Effectiveness of the developed approach is provided by special procedures and measures some of them are listed below:

- conservative system of Euler equation is integrated by fast implicit method;
- Chimera grid-embedding technique simplifies the problem of grid generation over complex configuration;
- second order finite volume cell centered Osher type flux difference scheme is used;
- effective Newton implicit solver based on approximate LU decomposition and GMRES algorithm provides very fast convergence;
- viscous wing wakes are calculated approximately by the two-dimensional Green's integral method;
- viscid-inviscid interaction including moderate separation regimes is determined by the quasi-simultaneous coupling scheme.

One of the main advantages of the developed solver TTHC is its high speed at acceptable accuracy. The computation time for real airplane configuration is approximately 2min (modern quad-core processor PC).

This paper describes the method and algorithm (TRAN-viscid) developed in TsAGI for taking into account specific responses of an elastic airplane in transonic flow. This numerical method simulates flow and geometrical complexities in more detail than the standard DLM. It belongs to the class of so called time linearized frequency domain CFD approaches for unsteady Euler equations. The aim was to introduce linearized Euler equations for aeroelastic analyses and to compare its result with standard potential theory methods like the DLM. Natural mode shapes are input to the TTHC as nodal displacements of the DLM aerodynamic grid, and then finite-difference solution of linearized unsteady Euler equations is conducted for each mode. The obtained pressure distribution is transformed to the same grid, in which modal shapes were specified in order to use traditional computational procedure for aeroelasticity analysis. The present work has been done in the direction of a development of the ARGON's methodology and software that will be used in TsAGI for multidisciplinary analysis and optimization in airplane design.

In the current paper the examples of aeroelastic applications of developed approach are represented. Computational results, which were received by the use of different CFD solvers are compared with the available experimental data for test cases of the LANN wing and the AGARD wing 445.6 configurations. Results of aeroelasticity analysis of the mid-range passenger airplane with high aspect ratio wing and the engine under the wing also are shown. Comparisons of aeroelasticity characteristics in transonic flow are presented for cases of linear (DLM) and nonlinear aerodynamic (TRAN-viscid and TRAN-inviscid) models. The main goal of the present work is to increase appreciably reliability of aeroelastic analysis results.

2 Small disturbance Euler method of transonic flow computation

The developed algorithm of time-harmonic characteristics calculation has been constructed on the basis of the small disturbance Euler equations technique used in the Blwf100 solver. The code Blwf100 was created for analysis of transonic flow over complex aerodynamic configuration taking into consideration the viscous effects on the wings including thin separation zones. The possible configurations are: body + arbitrary number of wings attached to a body + arbitrary number of nacelles. An

interference of the elements is also modeled (Fig. 1).
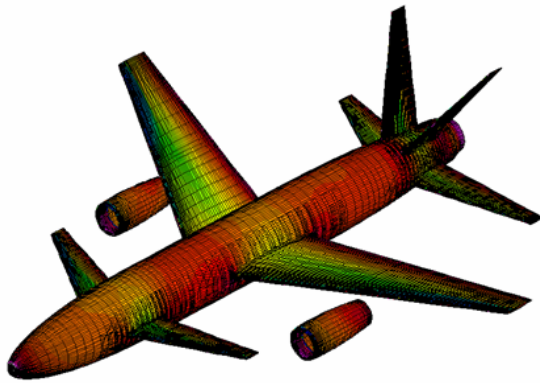
Fig. 1. Possible airplane configuration (Blwf100 code)

A viscous-inviscid interaction procedure is in the frame of the boundary layer theory. The calculation of the external inviscid steady flow is performed by a numerical integration of a conservative system of the Euler equations by fast implicit method and using the Chimera grid-embedding technique, which simplifies the problem of computational grid generation over complex configuration. The second order finite volume cell centered differentiable Osher type flux difference scheme is used. Effective Newton like implicit solver based on approximate LU decomposition and GMRES algorithm provides very fast convergence.

The laminar and turbulent compressible three-dimensional boundary layers are computed by a finite difference method using a predictor-corrector scheme applied to the Keller formulation. The equilibrium algebraic turbulence model is used. The boundary layer in the separated regions is determined by the inverse procedure. The viscous wing wakes are calculated approximately by the two-dimensional Green's integral method. It allows one to take into account the expected boundary layer response to the chordwise velocity variation and provides an effective and rapid computation of viscid-inviscid interaction. Comparison of computed steady pressure distribution with experimental data for LANN wing (AGARD configuration) is shown in Fig.2. Results are in a good agreement.
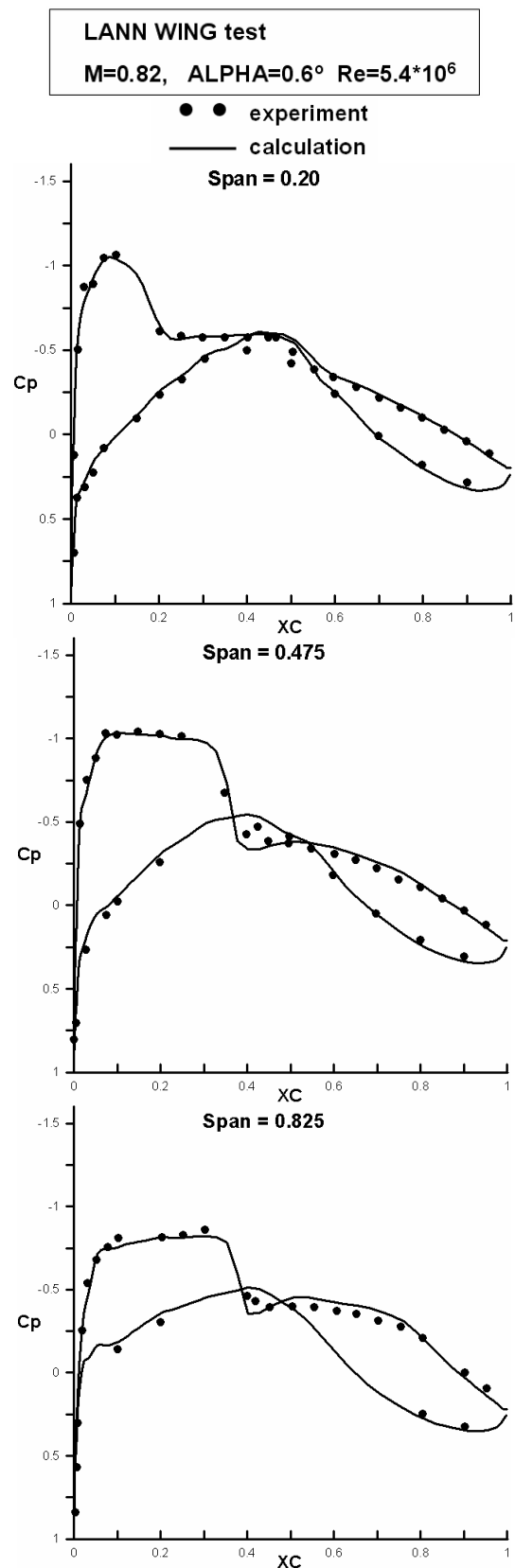
Fig. 2. Comparison of steady pressure distributions for LANN wing

The transonic time-harmonic calculation code (TTHC) has the same structure as BLWF100, uses the same algorithmic elements and can be applied for analyzing the similar complex configuration. The spatial disturbed fluxes are calculated on the basis of Euler fluxes linearization in the assumption that the local entropy does not change. The resulting system is conservative and linear one. The prescribed harmonic oscillations of an airplane are simulated by the corresponding flow transpiration on the undisturbed surface. An additional transpiration models the boundary layer response to the flow disturbance. As the resulting system of finite-difference equations of time-harmonic problem is linear, the solver provides the fast convergence of the iteration process. Unsteady pressure distribution results of computations and experimental data for LANN wing are compared in Fig. 3.
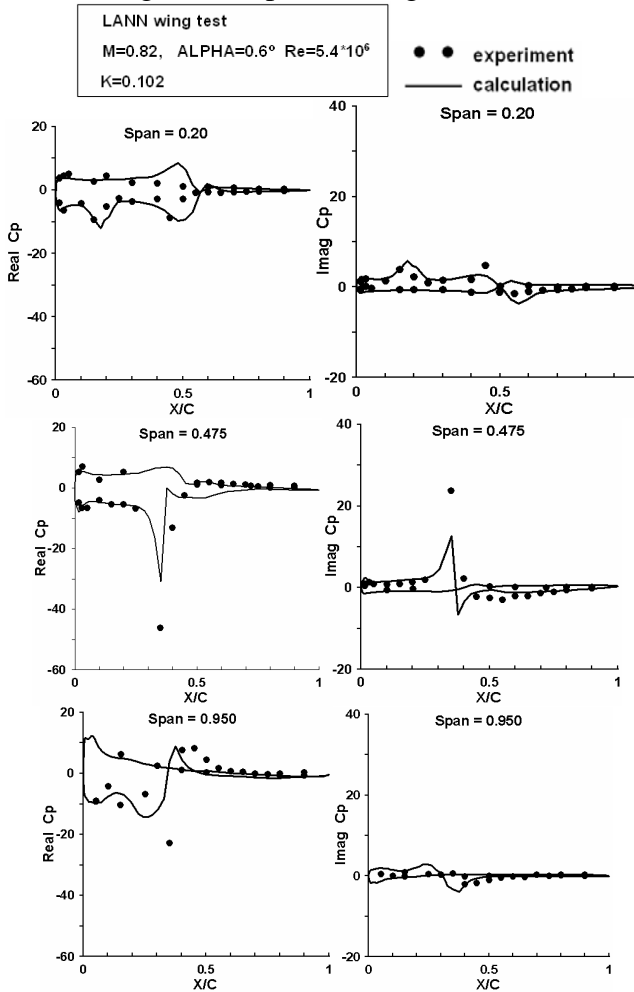
Fig. 3. Comparison of unsteady pressure distributions for LANN wing

Fig. 3 shows acceptable correspondence for the case of the wing oscillations in transonic flow with partly separated boundary layer.

One of the main advantages of the solver in the TTHC is its high speed at acceptable accuracy. The computation time for real airplane configuration is approximately 2min (modern quad-core processor PC).

3 Application of the small disturbance Euler equations for aeroelastic analysis

Equations of elastic airplane oscillations in the frequency domain are presented in the following form:

$$\left(-\omega^2 C + j\omega D_0 + G\right)q = Q^a + R\delta_c \qquad (1)$$

where q is a vector of modal generalized coordinates,

C, D_0, G are matrices of inertia, structural damping and stiffness,

Q^a is vector of modal aerodynamic generalized forces,

δ_c is a vector of control signals on actuators of control surfaces, and R is a matrix of controls transformation.

In the case of linear aerodynamics a vector of modal generalized forces can be presented as:

$$Q = -\left(\rho V j\omega D + \rho V^2 B\right)q \qquad (2)$$

where ρ, V are a density and velocity of flow, D, B are matrices of aerodynamic damping and stiffness, which depend on Mach number and reduced frequency.

It is supposed that modal analysis has been performed, flutter with linear aerodynamics has been studied, and a set of natural modes, which determine flutter characteristics, has been chosen (15-25 modes for symmetrical or antisymmetrical cases for complete airplane).

A set of reduced frequencies is also determined on the basis of linear flutter analysis (in general 5-7 values are sufficient).

Natural mode shapes are input to TTHC as nodal displacements f_x, f_y, f_z of DLM aerodynamic grid. Modal shape is determined by the displacements of 4 corners of each panel for the lifting surfaces (wing, horizontal tail,

4

vertical tail), and by the displacements of the nodes of central line for bodies (fuselage, nacelle) as beam deformations. Torsion of fuselage and nacelle does not result in aerodynamic forces.

Finite-difference solution of linearized unsteady Euler equations is conducted for each mode and each reduced frequency and the complex amplitudes of flow parameter oscillations are determined. Obtained pressure distribution is transformed to the same grid in which modal shapes were specified in order to aeroelasticity analysis could be conducted with the use of the same methods and computational procedure as for linear aerodynamics. The following data are obtained as a result of TTHC execution:

- A distribution of real and imaginary parts of nondimensional pressure difference in panel nodes – for lifting surfaces

$$\Delta c_{Pm} = \Delta c_{Pm}^{R}(x,z) + j\,\Delta c_{Pm}^{I}(x,z)$$

- A pressure distribution for body is integrated upon the surface of unitary length and is represented as two complex (vertical and horizontal) components

$$\Delta c_{Pym} = \Delta c_{Pym}^{R}(x) + j\,\Delta c_{Pym}^{I}(x)$$

$$\Delta c_{Pzm} = \Delta c_{Pzm}^{R}(x) + j\,\Delta c_{Pzm}^{I}(x)$$

Such approach is connected with the fact that in general a beam deformation is sufficient for airplane aeroelasticity problems, and local shell deformations are studied in other tasks. Here m is mode number, x,z are coordinates in lifting surface plane.

For aeroelastic applications modal generalized aerodynamic forces are determined using computed pressure distributions. They are defined by the formula

$$Q_m = \frac{\rho V^2}{2} \iint f_m\,\Delta c_P(x,z)\,dx\,dz$$

where f_m is the modal component normal to the lifting surface.

Pressure difference Δc_P is represented as a superposition of computed above modal pressure distributions Δc_{Pn}:

$$\Delta c_P = \sum_{n=1}^{N} \Delta c_{Pn}\,q_n\,.$$

The integration is then replaced by sum of mean values of pressure and displacement. The summation is conducted by different ways for lifting surfaces and bodies:

$$Q_m = \frac{\rho V^2}{2} \sum_{n=1}^{N} \left(\sum_{l=1}^{L_{LS}} f_{ml}^{LS}\Delta c_{Pnl}\,S_l + \sum_{l=1}^{L_B} f_{myl}^{B}\Delta c_{Pynl}\,\Delta x_l \right.$$
$$\left. + \sum_{l=1}^{L_B} f_{mzl}^{B}\Delta c_{Pznl}\,\Delta x_l \right) q_n$$

Here S_l is an area of panel of lifting surface ($l=1,\ldots,L_{LS}$),

f_{ml}^{LS} is a displacement component (normal to lifting surface) for m-mode and l-panel,

Δx_l is a distance between nodes along central line of body ($l=1,\ldots,L_B$)

f_{myl}^{B}, f_{mzl}^{B} are vertical and horizontal components of displacement of central line of body for m-mode and l-part of body.

The right part of Eq. (1) in transonic case in linear form as Eq. (2) is obtained by extracting real and imaginary parts of generalized force Q_m. Then standard aeroelasticity analysis procedure has been applied as for linear analysis. An algorithm similar to known PK-method is used for flutter calculation.

4 Test case: AGARD wing 445.6

The AGARD wing 445.6 is frequently used as the test case for comparison of results of computational methods and experiment since flutter measurements are available for a wide range of Mach numbers [7].

The linear structural model for the 445.6 wing was created in ARGON system using the wing model parameters presented in [7]. The wing is modeled with two bending beams and two torsion beams with the given stiffness and mass distribution.

The comparative results are given in Fig. 5 for the variant "2.5 foot weakened wing model 3 at zero angle of attack in air". Four first vibration modes were taken for calculations. Their natural frequencies are listed in the following table below:

No	f, Hz NASA	f, Hz TsAGI	Mode
1	9.6	9.56	1-st bending
2	38.16	38.09	1-st torsion
3	48.34	48.15	2-nd bending
4	91.54	92.04	2-nd torsion

The flutter analysis in ARGON was conducted in the frequency domain.

The non-dimensional flutter speed index for each Mach number was computed using the developed TRAN-viscid method, which is based on the Euler equations with taking into account a viscosity model (TTHC code). Figure 4 gives results from this method (green square symbols) and includes results from other studies (brown line: TRAN-inviscid [8]) for comparison. The TRAN-viscid results for Mach numbers below one are in good agreement with experiment. It can be seen that linear aerodynamics flutter calculations for this case are also in very good agreement with the experimental results except at M=0.96. This is to be expected, since nonlinear transonic effects.
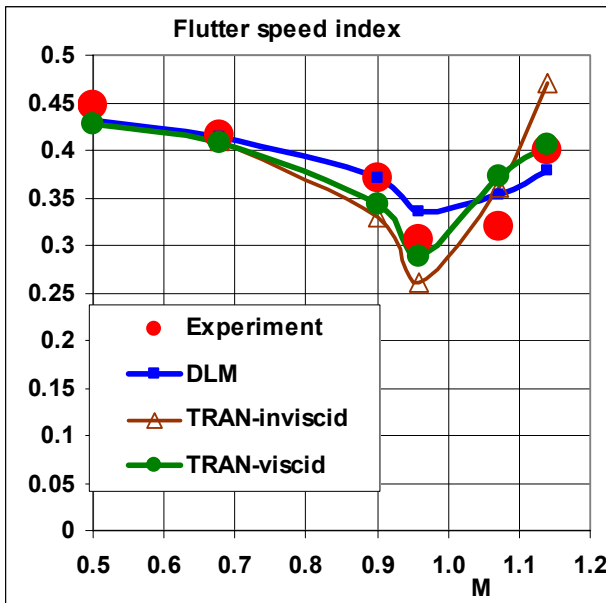
Fig. 4. Flutter boundaries for AGARD wing 445.6

The inviscid calculations based on nonlinear Euler equations [8] for $M = 0.901$ and 0.96 are appreciable lower than experimental transonic flutter dip. The results of TRAN-inviscid method are represented for the amplitude of flutter mode shape, corresponding to torsion angle on the wing tip: 1 degree. In the iterative TRAN-inviscid method [8] unsteady

aerodynamic coefficients are computed with taking into account both the shock movement and its intensity changes caused not only by the shock displacement but also by its velocity. At $M = 0.96$ the viscous calculation, from TRAN-viscid method, indicates that viscous modeling is required to correct these results. The discrepancy between experimental data and the nonlinear inviscid Euler code is certainly due to the presence of the viscosity in the flow. A number of factors may be considered in discussing the discrepancy. The flutter boundary for this model is quite sensitive to Mach number. In addition, for these Mach numbers, wind tunnel interference effects may be significant. Out of the transonic dip the discrepancies between linear, viscid and inviscid Euler codes and experiment are not very big.

5 Test case: medium range airplane

Aeroelasticity problems for different disciplines in transonic flow can be solved by developed method. Algorithms and programs are almost the same as in the case of linear aerodynamics. Static aeroelasticity, flutter and frequency response analysis have been considered below. As an example the medium range airplane (MRA) is used; the computational model of MRA is shown in Fig. 5.
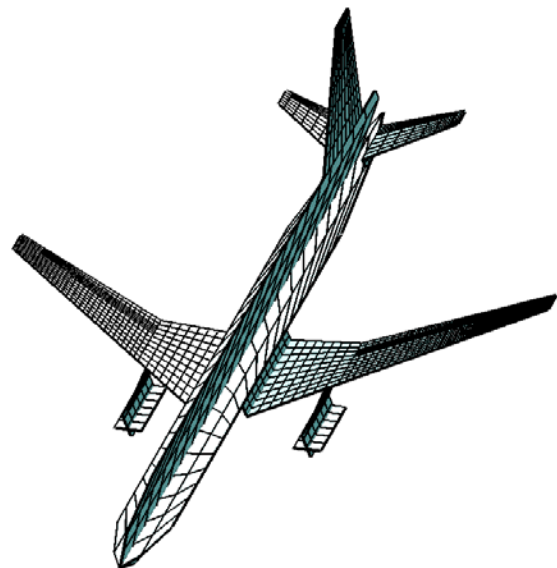
Fig. 5. Aerodynamic model of MRA for DLM

The AGON computational model of MRA consists of thin, initially flat elastic surfaces which coincide in form with the middle plates of the aggregates. The Ritz approach is used: the structural displacements of aircraft components are represented as a polynomial function of spatial coordinates.

For representation of elastic-mass properties of the airplane 5 elastic surfaces are used: Fuselage, Wing, Engine with a pylon, Horizontal tail, Vertical tail

The fuselage and the wing are assumed to bend in horizontal and vertical planes and to get torsion. Elastic deformations of the engine and pylon are not taken into account. For other elastic surfaces, beam schematization with bending in the normal plane and the torsion is used. Among themselves elastic surfaces are connected by 6-degree springs of rather large stiffness. Oscillations of the engine on a pylon are simulated with the aid of compliance of the spring connecting the pylon to the wing spar.

The total number of degrees of freedom of the polynomial Ritz method (on half of the structure) is 70 at calculation of symmetrical deformations, and 87 at calculation of anti-symmetrical deformations.

Mass distribution corresponds to the total mass of the airplane about 75 tons at the mass center position $x_{c.m.}$=20m from the nose of the airplane.

5.1 Static aeroelasticity

In the case transonic aerodynamics static aeroelasticity characteristics are determined on the basis of equations of motion in modal coordinates. As was mentioned above the elements of aerodynamic matrices B and D in (2) depend on Mach number and reduced frequency. Small values of reduced frequency (for example, k=0.001) are used for static aeroelasticity analysis.

The main features of transonic aerodynamic coefficients of considered MRA are shown in Figs. 6-8. The derivatives of the lift coefficient with respect to angle of attack and aileron deflection decrease abruptly at Mach number increase above 0.85 (cruise value M=0.82) as can be seen in Figs 6, 7. In addition,

the influence of structural elasticity on aerodynamic derivatives is considerably higher in transonic flow as can be seen from the ratio of derivatives of flexible and rigid airplane (Fig.8). This is caused by the shift of the aerodynamic center to the trailing edge in transonic flow. The dynamic pressure of the aileron reversal on lift decreases approximately on 20%.
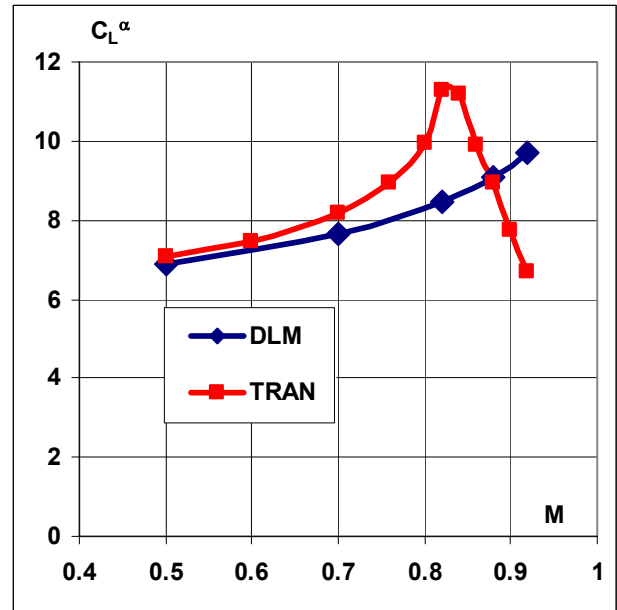
Fig. 6. Comparison of C_L^{α} for DLM and transonic code
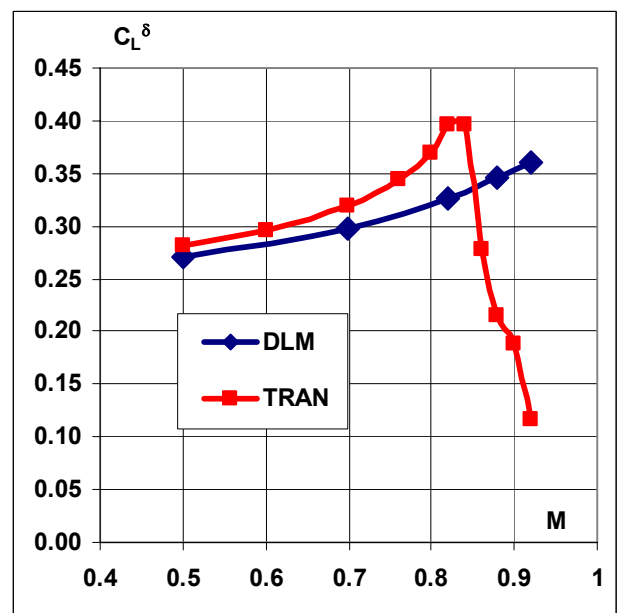
Fig. 7. Comparison of aileron effectiveness on lift for DLM and transonic code
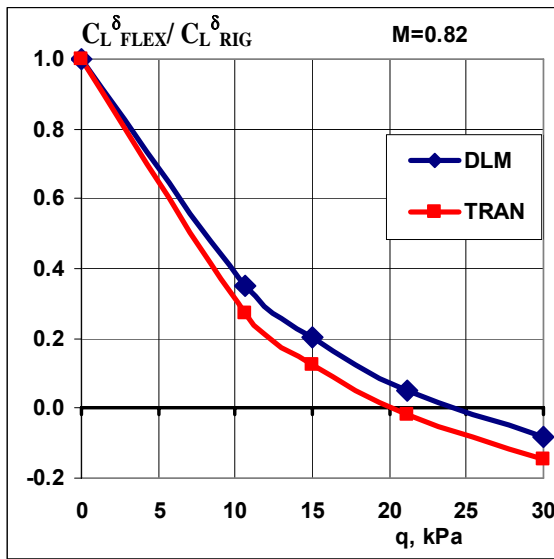
Fig. 8. Comparison of aileron effectiveness on lift for DLM and transonic code in dependence on dynamic pressure for cruise Mach number M=0.82

5.2 Flutter

Figures 9 and 10 show the dependencies of damping coefficients and frequencies of symmetrical elastic oscillations on the flow velocity in the case of linear and transonic aerodynamics at cruise Mach number M=0.82. Two flutter forms take place in both cases. The first form is connected with the engine pitch and wing bending vibrations (Flutter 4Hz). The second form is connected with the wing horizontal and vertical bending and torsion of the wing tip (Flutter 8Hz). The damping and frequency dependencies on flow velocity are in qualitative agreement. The lowest flutter speeds are practically the same, but the flutter speed of the second form is higher on 10% for transonic flow.

There are different features of the flutter boundaries for two flutter forms (Fig. 11). The first form demonstrates traditional transonic deep near Mach number M=0.76 unlike the DLM. The decrease of the second flutter speed is insignificant. At low Mach numbers the two aerodynamics give close results. Flutter frequencies also show different dependencies on Mach number (Fig. 12).
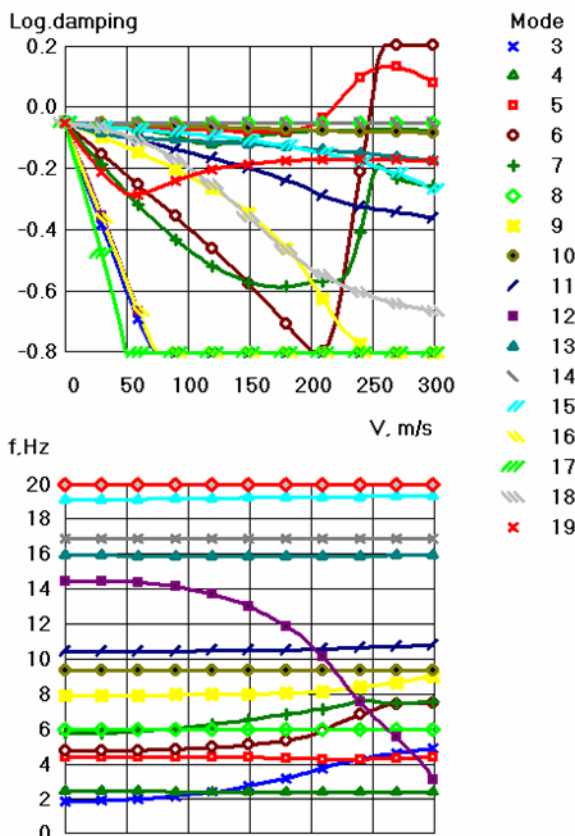
Fig. 9. Flutter V-g Plot for M=0.82, DLM
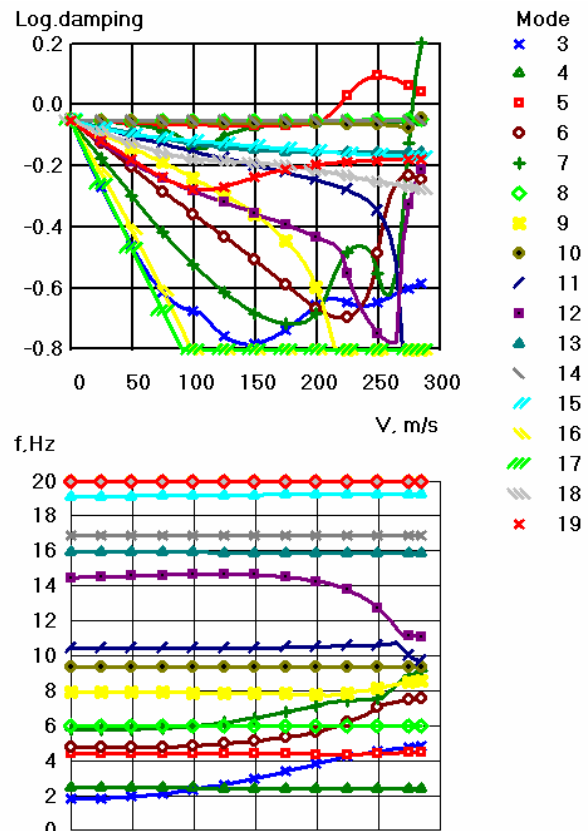
Fig. 10. Flutter V-g Plot for M=0.82, transonic code
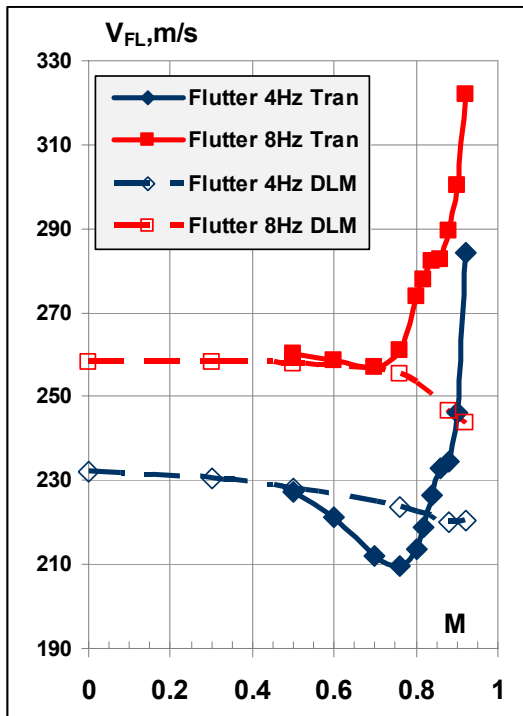
Fig. 11. Flutter speed versus Mach number
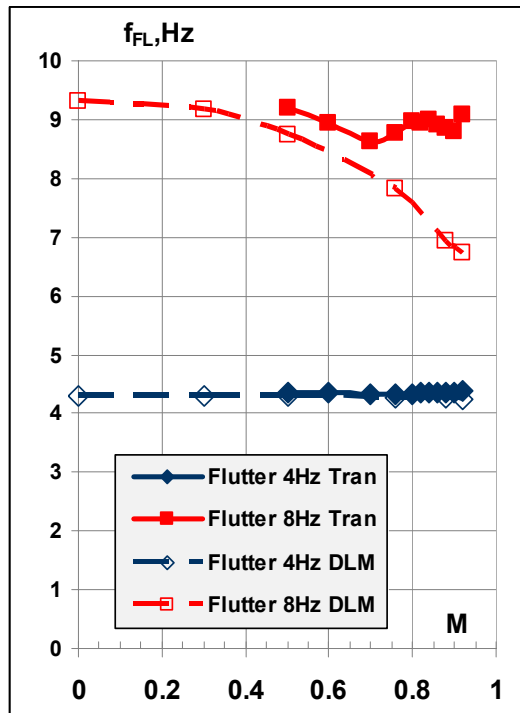
Fig. 12. Flutter frequency versus Mach number

5.3 Frequency response

Frequency response function (FRF) calculations are performed on the basis of equation (1) with using of an interpolation of elements of aerodynamic matrices on reduced frequency.

The comparison of FRF of the wing root bending moment due to symmetrical harmonic deflection of aileron for DLM and transonic aerodynamics is shown in Fig. 13 (cruise flight). Such type of FRF is used in development and analysis of effectiveness of maneuver and gust load alleviation systems. Figure 13 shows that phase FRF for both cases are very close in the frequency range up to 20Hz, but amplitude responses differ significantly. The response is almost twice higher for the case of transonic aerodynamics in low frequency range, and on the contrary it is several times lower in the high frequency range. This important for practice difference requires further investigations.
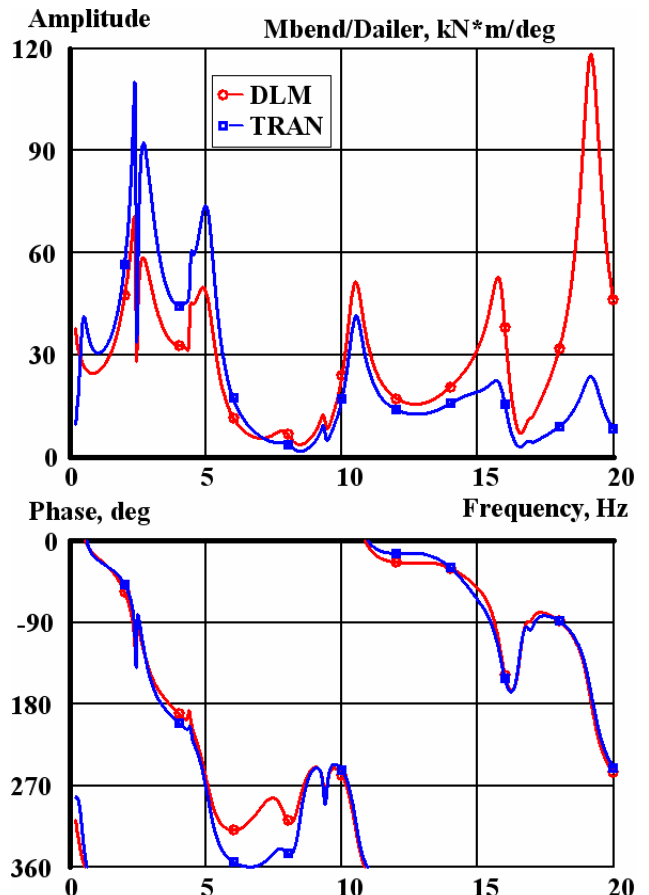
Fig. 13. Wing root bending moment due to aileron harmonic oscillations (M=0.82)

Another FRF – the pitch rate at flight control system (FCS) transducer location due to elevator harmonic oscillations – is presented in Fig. 14. Such type of FRF has significant importance for providing the required characteristics of the airplane stability and

controllability in flight dynamics and also for providing aeroservoelastic stability of the airplane with FCS. Here it can also be seen the appreciable exceeding of the response in the case of transonic aerodynamics in the low frequency range.
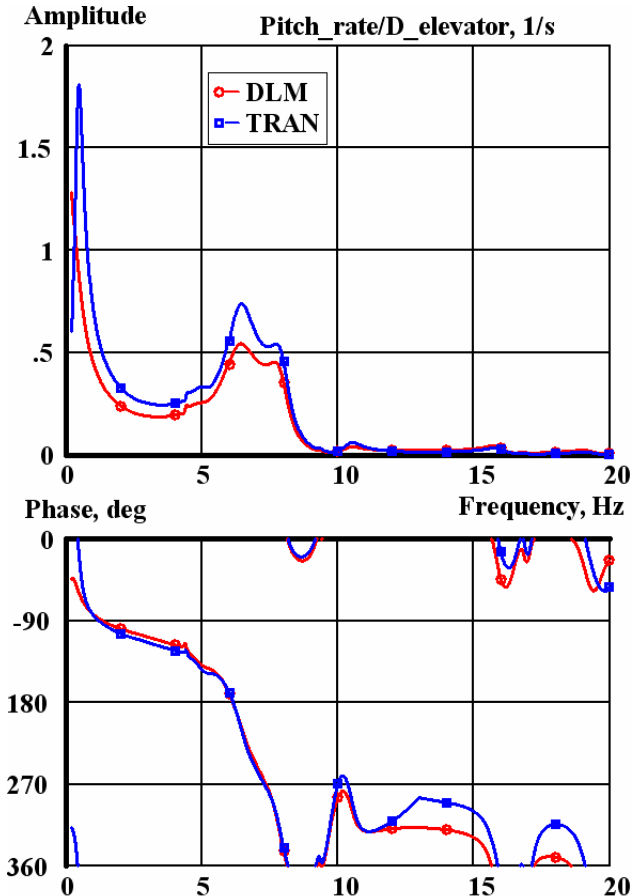
Fig. 14. Pitch rate at flight control system transducer location due to elevator harmonic oscillations (M=0.82)

Conclusion

Linear aeroelasticity analysis in AGON system is supplemented with an effective algorithm/procedure of aerodynamics computation using time-harmonic solutions of the Euler equations in transonic viscous flow. It is available for rather complex airplane configurations.

The present work has been done in the direction of the development of the ARGON's methodology and software, which are used for multidisciplinary analysis and optimization in airplane design.

Acknowledgement

References

[1] Edwards J.W. Computational Aeroelasticity. *Chapter 7 in Flight-Vehicle Materials, Structures and Dynamics, Vol. 5: Structural Dynamics and Aeroelasticity, American Society of Mechanical Engineers*, New York, 1993.

[2] Voss R. Numerical Simulations of Limit Cycle Oscillations in Transonic Airfoil Flow with Mild Separation. *Proceedings of CEAS/AIAA/AIAE International Forum on Aeroelasticity and Structural Dynamics (IFASD)*, Madrid, 2001.

[3] Henke H. H. Progress of the Viscous-Coupled 3D Euler Method EUVISC and Its Aeroelastic Application. *International Forum of Aeroelasticity and Structure Dynamics (IFASD)*, Amsterdam, 2003.

[4] Widhalm M., Dwight R. P., Thormann R. & Hübner A. Efficient computation of dynamic stability data with a linearised frequency domain solver. *In Proc. 5th Europ. Conf. Comp. Fluid Dyn. ECCOMAS-CFD*, Lisbon, 2010.

[5] Voss R., Brendes G. Separation. *Proceedings of CEAS/AIAA/AIAE International Forum on Aeroelasticity and Structural Dynamics (IFASD)*, Madrid, 2001.

[6] Palacios R., Climent H., Karlsson A., and Winzell B. Assessment of strategies for correcting linear unsteady aerodynamics using CFD or experimental results. *IFASD*, Madrid, 2001.

[7] Yates C. AGARD Standard Aeroelastic Configurations for Dynamic Response: I − Wing 445.6. *AGARD Report No.765*, July 1988.

[8] Kuzmina S. I., Ishmuratov F. Z., Mosounov V. A., Theoretical study of transonic flutter / buzz in the frequency and time domain. *ICAS-98-4,9,2*, Melbourne, 1998.

Copyright Statement